Catalysis Science & Technology

PAPER

View Article Online
View Journal | View Issue

Cite this: *Catal. Sci. Technol.*, 2019, **9**, 6965

Palladium doping of In_2O_3 towards a general and selective catalytic hydrogenation of amides to amines and alcohols†

Iván Sorribes, *[a] Samantha C. S. Lemos,[b] Santiago Martín, [c] Alvaro Mayoral, [d] Renata C. Lima [b] and Juan Andrés *[a]

Received 3rd September 2019,
Accepted 10th November 2019

DOI: 10.1039/c9cy02128k

rsc.li/catalysis

Herein, the first general heterogeneous catalytic protocol for the hydrogenation of primary, secondary and tertiary amides to their corresponding amines and alcohols is described. Advantageously, this catalytic protocol works under additive-free conditions and is compatible with the presence of aromatic rings, which are fully retained in the final products. This hydrogenative C–N bond cleavage methodology is catalyzed by a Pd-doped In_2O_3 catalyst prepared by a microwave hydrothermal-assisted method followed by calcination. This catalyst displays highly dispersed Pd^{2+} ionic species in the oxide matrix of In_2O_3 that have appeared to be essential for its high catalytic performance.

Introduction

The reduction of carboxylic acid derivatives is a fundamental reaction widely applied to exploratory organic chemistry in research laboratories as well as to industrial scale chemical production.[1] In particular, the reduction of amides yields a vast number of useful bulk platform chemicals and fine-synthesis intermediates for the preparation of dyes, pigments, agrochemicals, pharmaceuticals and other materials.[2] For instance, amine functionalities, which are essential motifs present in many bio-active compounds, are often constructed by initial amide formation followed by reduction.[3] In this context, a promising route for carbon dioxide valorization involving formamides as reaction intermediates is also noteworthy.[4]

Traditionally, amide reduction reactions have been carried out using (over)stoichiometric amounts of classical reagents such as lithium aluminum hydride ($LiAlH_4$) or boranes (B_2H_6), which require tedious workup procedures and generate large amounts of waste.[5] Recently emerged non-catalytic protocols using samarium iodide (SmI_2)/amine/H_2O,[6] sodium dispersions with different proton donors,[7] or sodium hydride (NaH) with zinc halides (ZnX_2; X = Cl, I)[8] have similar limitations. Different catalytic strategies have been developed for the reduction of amides to amines under hydrosilylation,[9] hydroboration[10] and transfer-hydrogenation[11] conditions, which are methodologies with wide applicability for functionalized amides, but they suffer from low atom-efficiency. In this respect, the catalytic hydrogenation of amides represents the most environmentally benign methodology, since water is formed as the only by-product.[12] However, as a result of the low electrophilicity of the carbonyl group, the catalytic reduction of amides with molecular hydrogen is a challenging reaction. In general, the hydrogenation of amides proceeds with the addition of a H_2 molecule to the carbonyl group to form an intermediate hemiaminal species.[2a,13] Subsequent elimination of H_2O and hydrogenation of the imine intermediate form an alkylated amine (deoxygenative reaction; Scheme 1, path A). In contrast, the C–N bond cleavage by collapse of the hemiaminal leads to the formation of the respective alcohol and deprotected amine products (deaminative reaction;

[a] *Departament de Química Física i Analítica, Universitat Jaume I, Av. Sos Baynat s/n, 12071 Castelló, Spain. E-mail: isorribe@uji.es, andres@uji.es*
[b] *Instituto de Química, Universidade Federal de Uberlândia, 38400-902, Uberlândia, MG, Brazil*
[c] *Departamento de Química Física, Facultad de Ciencias, Instituto de Ciencias de Materiales de Aragón (ICMA), Universidad de Zaragoza-CSIC, 50009 Zaragoza, Spain*
[d] *Center for High-resolution Electron Microscopy (ChEM), School of Physical Science and Technology, ShanghaiTech University, 393 Middle Huaxia Road, Pudong, Shanghai, 201210, China*

† Electronic supplementary information (ESI) available: General information, additional tables, schemes, figures, characterization data and NMR spectra of isolated products. See DOI: 10.1039/c9cy02128k

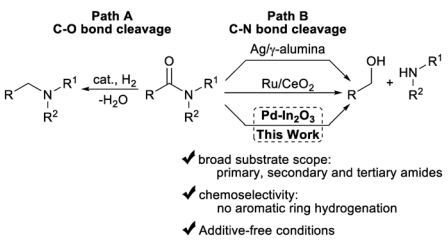

Scheme 1 Reaction pathways for the hydrogenation of amides and deaminative hydrogenation over heterogeneous catalysts.

Scheme 1, path B). Both reductive processes are potentially useful because of the importance of the products obtained and, interestingly, the C–N bond cleavage pathway may also be exploited as a selective deprotection methodology in organic synthesis. Moreover, this latter hydrogenative transformation is also relevant to H_2-storage systems based on alcohol/amide pairs as liquid organic hydrogen carriers.[14]

The deoxygenative reaction is a typical route for heterogeneous systems. Early catalysts based on copper–chromium oxides,[15] ReO_3,[16] RANEY® catalysts,[17] PtO_2,[18] and Pd–Re/high surface area graphite (HSAG)[19] catalyzed the hydrogenation of amides to amines under harsh conditions. Mitigation of reaction conditions was accomplished by applying more efficient bimetallic/bifunctional Rh–Re,[20] Ru–Mo,[21] Rh–Mo,[22] Ru–Re,[23] Pt–Re/TiO_2,[24] Pd–Re/graphite,[25] Rh/MoO_x–SiO_2, Ni/LaAlSiO,[26] Pt/Nb_2O_5,[27] Pt/MoO_x–TiO_2[27] and Ir/Mo-mesoporous SiO_2 (KIT-6)[28] catalysts. With this aim, a large screening of bi- and trimetallic systems was also performed, which allowed the identification of a relatively active catalyst based on Pt–Re–In supported on silica (or carbon).[29] Nevertheless, the most significant breakthrough to date has been recently reported, almost at the same time, by the groups led by Kaneda and Shimizu, who applied V-decorated Pt nanoparticles impregnated on hydroxyapatite (HAP)[30] and Re-loaded TiO_2,[31] respectively, as catalysts for the hydrogenation of amides *via* C–O bond cleavage (path A), while inhibiting arene hydrogenation. Since aromatic rings often structurally compose many of the amines used in life science applications, these processes represent important contributions to the synthetic chemist's toolbox, on both an academic and an industrial scale.

Alternatively, some elegant homogeneous approaches using Ru,[32] Ir[33] and Mn[34] pincer complexes in combination with specific Brønsted or Lewis acid co-catalysts have also been disclosed for the hydrogenation of amides to their corresponding alkylated amines, which fully retained the aromaticity. In contrast, the use of homogeneous catalysts is usually associated with the preparation of the respective alcohols and amines after C–N bond hydrogenolysis.[35] Although these processes operate under relatively mild conditions, the activity of most of these catalysts relies on metal–ligand cooperation and frequently entails the need for basic additives and synthetically complex ligands. Moreover, homogeneous catalytic systems imply other drawbacks associated with the difficulty involved in catalyst recovery and recycling. Advantageously, the use of heterogeneous catalysts represents a more convenient approach from a practical point of view.

To the best of our knowledge, there are only two examples on the hydrogenation of amides to alcohols and amines mediated by heterogeneous catalysts (Scheme 1). Recently, Milstein *et al.* have demonstrated that it is possible to carry out this C–N bond cleavage reaction by applying a heterogeneous catalytic system based on silver/γ-alumina.[36] However, the scope is mainly limited to secondary amides, showing moderate to low yields for primary and tertiary substrates. Although this heterogeneous catalyst does not promote the hydrogenation of aromatic moieties, it requires an excess of strong bases (such as potassium *tert*-butoxide) to ensure good activity after long reaction times (2–5 days). Shortly after, Tomishige and Tamura *et al.* reported the use of a heterogeneous CeO_2-supported Ru catalyst for the selective hydrogenation of the C–N bond in primary amides.[37] This reaction has been demonstrated in a narrow substrate scope, and its use is limited to aliphatic amides, since the unwanted aromatic ring hydrogenation occurs as a major side reaction. Nowadays, there is no heterogeneous catalyst capable of performing the hydrogenation of primary, secondary and tertiary amides in the absence of exogenous additives with concomitant C–N bond cleavage to furnish alcohols and amines containing both aromatic and aliphatic moieties. Hence, the development of more efficient and selective heterogeneous catalysts for amide hydrogenation reactions *via* C–N bond cleavage under more environmentally benign conditions is currently highly desirable.

Herein, we describe the preparation of Pd-doped In_2O_3-based catalysts by a microwave hydrothermal-assisted method combined with a rapid post-thermal treatment. We demonstrate their performance in the hydrogenation of primary, secondary and tertiary amides to alcohols and amines, establishing the first general and selective heterogeneous catalytic protocol for this reaction that works under additive-free conditions and is compatible with the presence of aromatic ring systems.

Results and discussion

Preparation and characterization of catalysts

In_2O_3-based materials have emerged as efficient catalytic systems for hydrogenation reactions including the conversion of CO_2 to methanol,[38] to CO (reverse water gas shift)[39] or to C_2–C_4 hydrocarbons,[40] the conversion of CO into light olefins,[41] and the semihydrogenation of acetylene.[42] In addition, recent density functional theory (DFT) simulations have suggested that In_2O_3 should also be a promising heterogeneous catalyst for the hydrogenation of acetic acid to ethanol.[43] In general, the experimental and theoretical[44] studies have revealed that oxygen vacancies, commonly formed under hydrogenative conditions,[45] play a crucial role in the adsorption and activation of the reactant molecules as well as in the stabilization of key intermediates during the reaction. Interestingly, the material properties of In_2O_3 can be modulated by doping with other metals.[46] More specifically, its hydrogenation activity can be enhanced by doping with Pd, which is claimed to facilitate hydrogen splitting and the creation of oxygen vacancies. In addition, the presence of Pd allows the generation of interfacial sites that have been proposed as active sites capable of activating the reactants, thus facilitating the hydrogenation reaction.[42a,47]

This background led us to hypothesize that Pd-doped In_2O_3 catalysts should be attractive candidates for the efficient hydrogenation of amides. The low electrophilic carbonyl

group of the amide could be activated *via* Lewis acid–base interaction with the oxygen vacancies (*i.e.* In^{n+} sites), while the required hydrogen dissociation should be accomplished by neighboring Pd species. Similar cooperative catalysis has been previously reported for homogeneous[3j,11,32b–f,33–35h] as well as heterogeneous catalytic systems.[24a,27,30–31]

Based on this premise, we attempted to prepare an active Pd-doped In_2O_3 catalyst for the hydrogenation of amides by a microwave hydrothermal-assisted method,[48] which is a well-established technique for the preparation of metal oxide precursors with a homogeneous distribution and control over their morphology,[46c,49] combined with a calcination treatment. To this end, aqueous solutions of In(III) acetate and variable amounts of Pd(II) chloride were adjusted to pH 12 and reacted in an autoclave under microwave heating at 140 °C. The final Pd-doped In_2O_3 materials were obtained by subsequent calcination at 400 °C for 2 min (see the Experimental section for details of the preparation). The Pd contents of the prepared materials were 1, 1.5, 3.5 and 5.3 wt%, as determined by inductively coupled plasma atomic emission spectroscopy (ICP-AES) analysis. In addition, for the sake of comparison the pure In_2O_3 material was also synthesized using the same preparation methodology.

Fig. 1a shows the X-ray diffraction (XRD) patterns of the pure In_2O_3 and Pd-doped In_2O_3 materials after the annealing treatment. All observed diffraction peaks were indexed to the crystalline body-centered cubic (bcc)-In_2O_3 structure (JCPDS card no 06-0416). No additional diffraction peaks associated with the presence of secondary phases were detected in the Pd-doped In_2O_3 materials, indicating that the synthetic methodology used allows for the insertion of Pd^{2+} ions into the In_2O_3 matrix without the formation of other Pd species. This insertion influences the long-range periodicity of the materials and also implies a decrease in their crystal size compared to pure In_2O_3 (Table S1 in the ESI†).

The substitution process of In^{3+} by Pd^2 should also entail local distortions in the oxide lattice, which can be detected by Raman-scattering measurements. The Raman spectra of the prepared In_2O_3 and Pd-doped In_2O_3 materials ranging from 105 to 700 cm^{-1} are depicted in Fig. 1b. All of them show the characteristic bands of the vibration modes of the (bcc)-In_2O_3 structure, which fully agree with the values reported in the literature.[50] The signals at 130, 306 and 366 cm^{-1} are related to the vibration of the O–In–O bending angle of the InO_6 octahedral units, as building blocks of the In_2O_3 lattice, while the peaks at 495 and 630 cm^{-1} are assigned to the stretching of the In–O bonds of these InO_6 octahedra. Interestingly, the peak located at 306 cm^{-1} is known to be correlated to the oxygen vacancies/defects within the lattice of In_2O_3.[51] A decrease in the crystallite size and the presence of local distortions, both associated with the existence of oxygen vacancies to a higher extent, produce the broadening of this Raman peak.[52] As shown in Fig. 1b (and Table S1 in the ESI†), in the Pd-doped In_2O_3 materials this Raman mode becomes broader with the increase of the Pd content, thus denoting a higher density of oxygen defects in these materials. Moreover, the creation of oxygen vacancies also provokes the weakness of the In–O bonds, which is reflected in the redshift of this Raman peak for the Pd-doped In_2O_3 materials.[53] It should be noted that no additional Raman modes, including those of Pd(II) oxide,[54] are observed for the Pd-doped In_2O_3 materials, thus denoting the absence of any impurity phase, which is in good agreement with the XRD analysis.

Fig. 2 shows the images obtained by transmission electron microscopy (TEM). The pure In_2O_3 and Pd–In_2O_3 (5.3 wt%) materials exhibit nanostructures with a homogeneous size distribution, which vary from 5 up to 20 nm, and a rounded shape morphology (Fig. 2a and b). High-resolution TEM analysis confirms the high crystallinity of the materials, being possible to visualize some of the planes associated with the (bcc)-In_2O_3 structure (insets of Fig. 2a and b). However, no Pd nanoparticles were detected in the Pd–In_2O_3 (5.3 wt%) material even by spherical aberration (Cs)-corrected HAADF-STEM analysis (Fig. 2d and e). In contrast, a uniform distribution of Pd can clearly be confirmed by energy-dispersed X-ray (EDX) elemental mapping (Fig. 2c), thus suggesting that Pd is atomically distributed along the structure of In_2O_3.

Catalytic results

Initial hydrogenation experiments were performed in toluene at 160 °C, under a pressure of 60 bar of H_2 and using benzanilide (**1**) as a model substrate. Under these conditions, catalyst Pd–In_2O_3 (5.3 wt%) afforded aniline (**2**) and benzyl alcohol (**3**) in 98 and 92% yields, respectively, with only traces (2% yield) of *N*-benzylaniline (**4**) as a by-product (Fig. 3b and

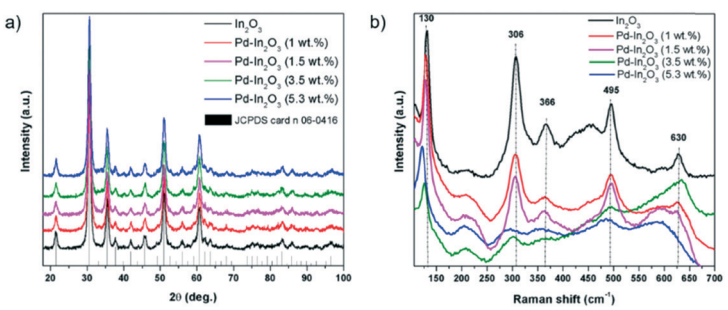

Fig. 1 (a) X-ray diffraction patterns of In_2O_3 and Pd-doped In_2O_3 catalysts. The vertical lines below the XRD patterns indicate the expected reflection positions of body-centered cubic (bcc)-In_2O_3. (b) Raman spectra of In_2O_3 and Pd-doped In_2O_3 catalysts.

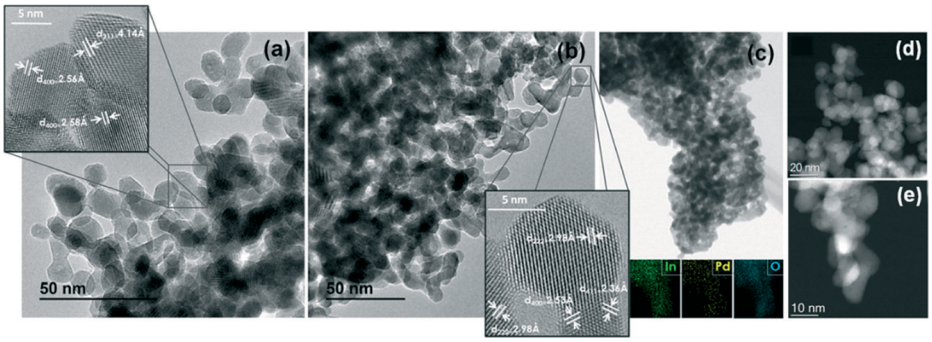

Fig. 2 TEM micrographs of (a) In_2O_3 and (b) Pd–In_2O_3 (5.3 wt%) catalysts. HRTEM images are shown in the inset. (c) STEM image and EDX elemental mapping of In, Pd and O for catalyst Pd–In_2O_3 (5.3 wt%). Low- (d) and high- (e) magnification images for the Cs-corrected HAADF-STEM analysis of catalyst Pd–In_2O_3 (5.3 wt%).

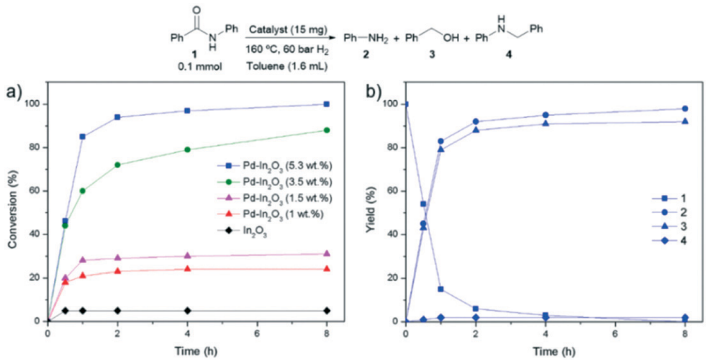

Fig. 3 (a) Benzanilide (**1**) conversion over In_2O_3 and Pd-doped In_2O_3 catalysts *versus* reaction time. (b) Yield–time curves for the hydrogenation of **1** in the presence of catalyst Pd–In_2O_3 (5.3 wt%).

Table 1, entry 1). Importantly, no ring-hydrogenated products were detected. Evaluation of Pd-doped In_2O_3 catalysts with different Pd contents showed that the initial reaction rate for the hydrogenation of **1** increases linearly with the Pd loading, while almost no reaction took place using pure In_2O_3 as a catalyst (Fig. 3a and Fig. S1 and S2 in the ESI†). These results demonstrate that the Pd site density plays a crucial role not only in the generation of oxygen vacancies to a higher extent (according to the Raman characterization), but also in the hydrogen activation, which is essential for achieving the hydrogenation of **1**.

Table 1 Hydrogenation of benzamide (**1**) catalyzed by Pd–In_2O_3 (5.3 wt%)[a]

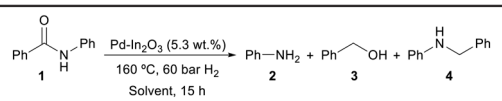

Entry	Solvent	Conversion[b] [%]	Yield[b,c] [%]		
			2	3	4
1	Toluene	>99	98 (90)	92 (84)	2
2[d]	Toluene	82	81	76	1
3[e]	Toluene	62	56	52	1
4[f]	Toluene	66	64	62	2
5[f]	THF	18	18	16	—
6[f]	1,4-Dioxane	20	17	16	—
7[f]	MeOH	2	2	1	—
8[f]	EtOH	2	2	2	—
9[f]	i-PrOH	12	11	10	—
10[f]	Me-cyclohexane	59	55	51	4
11[f]	*n*-Hexane	58	55	52	3

[a] Reaction conditions: **1** (0.1 mmol), catalyst (15 mg), solvent (1.6 mL), 60 bar H_2, 160 °C, 15 h. [b] Determined by GC using *n*-hexadecane as an internal standard. [c] Yield of isolated product starting from 5 mmol of **1** shown in parentheses. [d] 30 bar H_2. [e] 15 bar H_2. [f] 130 °C.

This hydrogenative reaction proceeds with high selectivity towards the formation of products **2** and **3** in moderate to good yields depending on the hydrogen pressure used (Table 1, entries 2 and 3). Temperature also affects the hydrogenation outcome since a lower activity was achieved at 130 °C (Table 1, entry 4). The screening of different solvents was carried out at this temperature (130 °C) in order to observe their possible positive effect on the reaction. However, while ether-based solvents, such as THF and 1,4-dioxane, provided considerably lower conversions, almost no reaction took place in the presence of alcohols, probably as a result of the partial or full blockage of the existing oxygen vacancies,[45] thus preventing the substrate–catalyst interaction (Table 1, entries 5–9). Indeed, similar results to those of toluene were afforded by using non-oxygenated solvents (Table 1, entries 10 and 11). Nevertheless, toluene remained the best among those tested, and therefore it was the solvent of choice for further catalytic studies.

Characterization of the recovered catalyst (Pd–In_2O_3 (5.3 wt%)-R1) by XRD after the hydrogenation reaction of the model substrate under the established reaction conditions (see Table 1, entry 1) demonstrated the preservation of the cubic (bcc)-structure In_2O_3 phase (Fig. S3 in the ESI†). Catalyst Pd–In_2O_3 (5.3 wt%)-R1 also preserves its high crystallinity with a homogeneous dispersion of Pd species as revealed by HRTEM and EDX elemental mapping (Fig. 4a and b). However, a thorough analysis by Cs-corrected HAADF-STEM denoted the formation of few and isolated Pd nanoparticles (below 5 nm) with an interlayer *d*-spacing of 2.31 Å associated with the {111} plane of Pd(0), denoting that some desorption of Pd species from the In_2O_3 backbone takes place during catalysis (Fig. 4c and d). It should be noted that the ICP-AES analysis of the reaction filtrate after catalyst separation confirmed that the content of Pd and In in solution was below the detection limit, which suggests that, after desorption, the Pd species agglomerate to form the metal nanoparticles.

In a second run, the recovered catalyst Pd–In_2O_3 (5.3 wt%)-R1 achieved a low conversion of benzanilide (30%) towards the formation of aniline and benzyl alcohol. Nevertheless, to our delight its catalytic activity could be efficiently recovered by a rapid (2 min) annealing treatment at 400 °C (see the ESI† for further details), which made possible the use of the catalyst for successive recycles with no significant loss of activity (Fig. 5).

To shed light on the catalyst deactivation/activation process, and therefore on the species involved during catalysis, X-ray photoelectron spectroscopy (XPS) studies of the fresh (Pd–In_2O_3 (5.3 wt%)), used (Pd–In_2O_3 (5.3 wt%)-R1) and reactivated (Pd–In_2O_3 (5.3 wt%)-R1–400) catalysts were performed. As shown in Fig. 6a, the In 3d core level spectrum of catalyst Pd–In_2O_3 (5.3 wt%) shows two peaks with electron-binding energy values of 443.4 and 451.0 eV, which are associated with the characteristic spin–orbit splitting of $3d_{5/2}$ and $3d_{3/2}$, respectively, and denote the presence of In(III) species. The Pd 3d spectrum also evidences a doublet peak, namely, the $3d_{5/2}$ and $3d_{3/2}$ peaks located at 336.1 and 341.5 eV, respectively (Fig. 6e). These peaks with a separation of 5.4 eV and an area ratio of 1.7 (63.1 and 36.9%, respectively) are associated with the presence of Pd(II). Interestingly, since other separated Pd(II)-containing phases were not detected by XRD and Raman analyses (Fig. 1), these results also confirm the insertion of Pd into the In_2O_3 matrix. In contrast, while the XPS spectrum of the used catalyst Pd–In_2O_3 (5.3 wt%)-R1 only shows in the In 3d region the characteristic doublet peak with the same separated spin–orbit components of 7.6 eV associated with In(III), the Pd core level spectrum shows four peaks after deconvolution and fitting (Fig. 6b and f, respectively). Two peaks are located at practically the same binding energies (336.6 and 342.1 eV), with the same area ratio (28.1 and 17.4%, respectively) and peak separation (5.5 eV) as those observed for the fresh catalyst Pd–In_2O_3 (5.3 wt%). In addition, a new doublet peak attributed to Pd(0) at 334.6 and 340.0 eV, with an area ratio of 1.6 (33.7 and 20.9%, respectively) and a peak separation of 5.4 eV, is also present (Fig. 6f). These results confirm the integrity of In(III) and the partial reduction of Pd(II) to Pd(0) species under reaction conditions, respectively. It should be noted that the absence of diffraction peaks associated with the presence of metallic Pd(0) species in the XRD pattern of the used catalyst Pd–In_2O_3 (5.3 wt%)-R1 (Fig. S3 in the ESI†) indicates that these species are highly dispersed on the In_2O_3 structure, as revealed by EDX elemental mapping, and to a minor degree, form agglomerated metallic nanoparticles (see Fig. 4b and d, respectively).

Under the annealing process at 400 °C, through which the catalyst recovers its catalytic activity, the Pd(0) species are completely oxidized to Pd(II), as confirmed in the Pd 3d core level spectrum of catalyst Pd–In_2O_3 (5.3 wt%)-R1-400 (Fig. 6h) by the presence of only two peaks with the same binding energies (336.1 and 341.5 eV), same peak separation (5.4 eV) and area ratio (1.7) as those observed for the fresh catalyst Pd–In_2O_3 (5.3 wt%). These results suggest that the reduction of Pd(II) to Pd(0) species might be the main reason for catalyst deactivation. Therefore, to obtain further confirmation on this assumption, the used catalyst Pd–In_2O_3 (5.3 wt%)-R1 was annealed at 250 °C to obtain a partially oxidized catalyst (Pd–In_2O_3 (5.3 wt%)-R1-250). As shown in Fig. 6g, the intensity of the peaks associated with Pd(0) in the XPS spectrum for the Pd 3d region of this catalyst is considerably lower than that for the used one, Pd–In_2O_3 (5.3 wt%)-R1 (Fig. 6f).

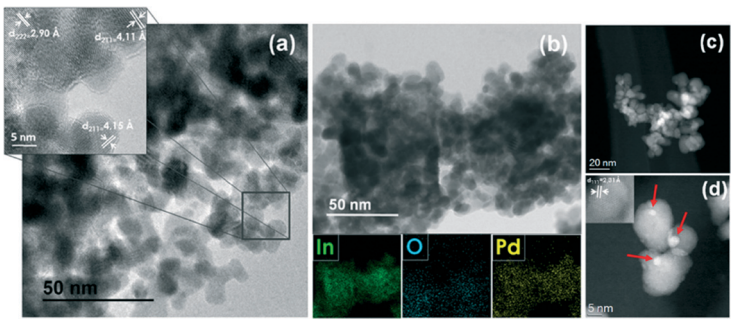

Fig. 4 (a) TEM micrograph of catalyst Pd–In_2O_3 (5.3 wt%)-R1. The HRTEM image is shown in the inset. (b) STEM image and EDX elemental mapping of In, O and Pd for catalyst Pd–In_2O_3 (5.3 wt%)-R1. Low- (c) and high- (d) magnification images for the Cs-corrected HAADF-STEM analysis of catalyst Pd–In_2O_3 (5.3 wt%). The red arrows point the generated Pd nanoparticles, and the lattice fringes are shown in the inset.

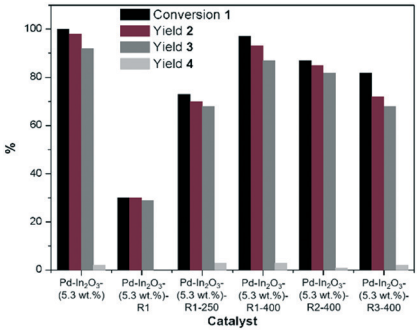

Fig. 5 Catalyst recycling experiments for the hydrogenation of benzanilide (**1**). Reaction conditions: **1** (0.2 mmol), catalyst (30 mg), toluene (3.2 mL), 60 bar H_2, 160 °C, 15 h.

Consequently, an enhanced catalytic activity was obtained in the presence of catalyst Pd–In_2O_3 (5.3 wt%)-R1-250, which achieved a good conversion of benzanilide (73%) with excellent selectivity towards the hydrogenative C–N bond cleavage affording aniline and benzyl alcohol in 70 and 68% yields, respectively (Fig. 5). Nonetheless, its catalytic activity is still lower than that of the fully oxidized catalyst Pd–In_2O_3 (5.3 wt %)-R1-400, thus demonstrating that the catalytic performance of these Pd–In_2O_3 catalysts is diminished when the relative content of Pd(0) is increased with respect to Pd(II) species in the In_2O_3 surface.

The O 1s core level spectrum of the fresh catalyst Pd–In_2O_3 (5.3 wt%) shows three peaks at 528.9, 530.7 and 532.9 eV after deconvolution, which can be ascribed to the lattice oxygen of In_2O_3, to oxygen defects (*i.e.* oxygen vacancies, in good agreement with the Raman characterization) and to adsorbed oxygen (O_2^-, O^-, OH^-, *etc.*), respectively (Fig. 6i). After the catalytic reaction, an increase of the relative oxygen vacancy concentration ($C_{Odefect}$) is observed in the used catalyst Pd–In_2O_3 (5.3 wt%)-R1, thus revealing that the reduction of the Pd species from Pd(II) to Pd(0) also implies the creation of an excess of oxygen vacancies in the oxide surface as a way to compensate for the charge difference (Fig. 6j). In line with the previously observed re-oxidation process, catalyst Pd–In_2O_3 (5.3 wt%)-R1-250 displays a decreased $C_{Odefect}$ compared to the used catalyst Pd–In_2O_3 (5.3 wt%)-R1 (Fig. 6k and j, respectively), while the catalyst obtained under the treatment at 400 °C (Pd–In_2O_3 (5.3 wt%)-R1-400) presents almost the same defect density as the fresh catalyst (Fig. 6l and i, respectively), which also evidences the successful recovery of the catalyst surface after the first activation process. However, in view of the slight progressive decrease of the catalytic activity observed with successive runs (Fig. 5), no total recovery of the original catalyst surface seems to take place after consecutive deactivation/activation processes, likely as a result of the desorption of Pd species from the In_2O_3 surface to a higher extent.

The general applicability of the catalyst Pd–In_2O_3 (5.3 wt%) was investigated by testing a broad range of primary, secondary and tertiary amides, including both aromatic and aliphatic moieties. The investigation of the substrate scope was performed at 160 °C and 60 bar of H_2 using toluene as the solvent for a standard reaction time of 15 h, while higher catalyst loadings were used to improve the conversion of the less reactive substrates (Table 2). Firstly, substituted benzanilides were hydrogenated, affording the corresponding aniline and benzyl alcohol derivatives in good to excellent yields (Table 2, entries 1–4). Benzanilides functionalized at the *N*-aryl group seem to be hydrogenated more easily than their benzoyl-substituted counterparts. The hydrogenation reaction could be efficiently accomplished in the presence of electron-donating groups, such as methoxy- or methyl-, as well as for fluoro-substituted benzanilides. For instance, 4-fluoro-*N*-phenylbenzamide was successfully hydrogenated, and aniline and 4-fluorobenzyl alcohol were afforded in 85 and 72% yields, respectively (Table 2, entry 4). However, the hydrogenation of benzanilides containing other electron-withdrawing functional groups, such as 4-chloro-*N*-phenylbenzamide, was reluctant (see Scheme S1 in the ESI†), thus revealing that the electronic properties of the substituents have an important

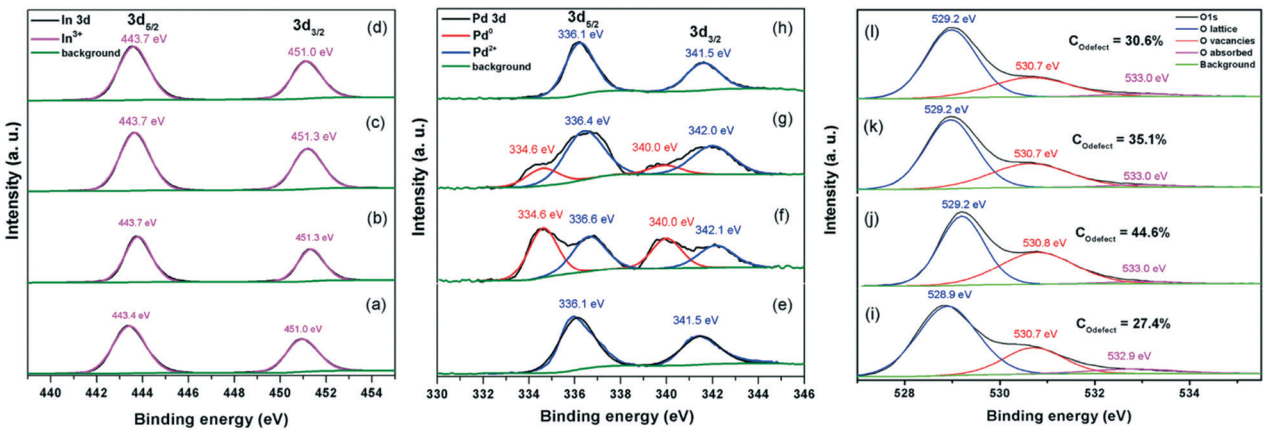

Fig. 6 In 3d, Pd 3d and O 1s XPS spectra of catalysts (a, e and i) Pd–In_2O_3 (5.3 wt%), (b, f and j) Pd–In_2O_3 (5.3 wt%)-R1, (c, g and k) Pd–In_2O_3 (5.3 wt %)-R1-250, and (d, h and l) Pd–In_2O_3 (5.3 wt%)-R1-400, respectively. $C_{Odefect}$ values were calculated according to ref. 47*d*.

impact on the catalytic performance of the catalyst Pd–In_2O_3 (5.3 wt%). The hydrogenation ability of this catalyst is not limited to *N*-aryl-substituted benzamides. Indeed, *N*,*N*-dimethylbenzamide was smoothly hydrogenated resulting in 95% yield of benzyl alcohol (Table 2, entry 5), and interestingly the hydrogenation of the most challenging primary benzamide could also be achieved in moderate conversion and high selectivity (Table 2, entry 6).

Next, a family of secondary and tertiary acetanilides were tested. *N*-Methyl-*N*-phenylacetamide, *N*-acetyl-1,2,3,4-tetrahydroquinoline and the more sterically hindered *N*,*N*-diphenylacetamide underwent hydrogenation to their corresponding secondary amines in quantitative yields (Table 2, entries 7–9). Acetanilide and its functionalized derivatives were also fully converted with excellent selectivity for C–N bond cleavage in the presence of an increased catalyst loading (Table 2, entries 10–16). Importantly, catalyst Pd–In_2O_3 (5.3 wt%) is also compatible with the presence of potentially reducing pyridine rings, which are typically present in important bioactive amides (Table 2, entry 17). Overall, these results

Table 2 Pd–In_2O_3 (5.3 wt%)-catalyzed hydrogenation of amides to amines and alcohols[a]

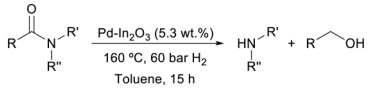

Entry	Amide	Conv.[b] [%]	Yield [%]		Entry	Amide	Conv.[b] [%]	Yield [%]	
			Amine[b,c]	Alcohol[b,c]				Amine[b,c]	Alcohol[b,c]
1	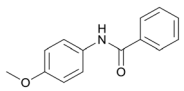	>99	>99 (90)	89 (82)	12[d,n]	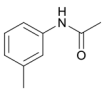	>99	97 (85)	88
2[d,e]	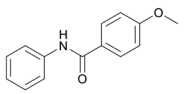	>99	95 (87)	86 (73)	13[l,o]	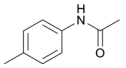	>99	95 (88)	86
3[f,g]	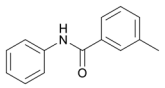	>99	97 (90)	90 (79)	14[l,p]	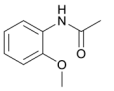	>99	98 (90)	90
4[f,h]	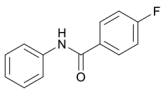	>99	85	71	15[d,q]	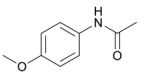	>99	87 (79)	76
5[i]	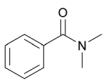	>99	n.d.	95 (85)	16[l,r]	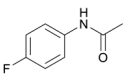	>99	93 (84)	83
6[j]	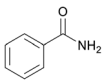	70	n.d.	62 (51)	17[j,s]	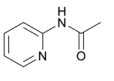	84	83 (72)	75
7	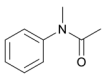	>99	>99 (91)	91	18		>99	36[t] 64[u]	—
8		>99	>99 (93)	93	19	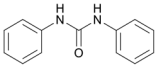	>99	67[t] 33[u]	—
9	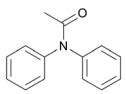	>99	>99 (95)	91	20		>99	>99	90
10[d,k]	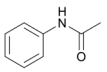	>99	97 (88)	86	21[v]	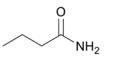	>99	n.d.	89
11[l,m]	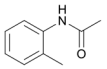	>99	98 (88)	88	22[v]	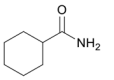	>99	n.d.	85 (76)

[a] Reaction conditions: amide (0.1 mmol), catalyst (15 mg), toluene (1.6 mL), 60 bar H_2, 160 °C, 15 h. [b] Determined by GC using *n*-hexadecane as an internal standard. [c] Yield of isolated product starting from 0.5 mmol of amide shown in parentheses. [d] Catalyst (30 mg). [e] *N*-(4-Methoxybenzyl)aniline (4%) and 1-methoxy-4-methylbenzene (3%) as by-products. [f] Catalyst (40 mg). [g] *N*-(3-Methylbenzyl)aniline (3%) as a by-product. [h] *N*-(4-Fluorobenzyl)aniline (14%) and benzyl alcohol (10%) as by-products. [i] Catalyst (20 mg). [j] Catalyst (60 mg). [k] *N*-Ethylaniline (2%) as a by-product. [l] Catalyst (35 mg). [m] *N*-Ethyl-2-methylaniline (2%) as a by-product. [n] *N*-Ethyl-3-methylaniline (2%) as a by-product. [o] *N*-Ethyl-4-methylaniline (4%) as a by-product. [p] *N*-Ethyl-2-methoxyaniline (2%) as a by-product. [q] *N*-Ethyl-4-methoxyaniline (12%) as a by-product. [r] *N*-Ethyl-4-fluoroaniline (6%) as a by-product. [s] *N*-Ethylpyridin-2-amine (<1%) as a by-product. [t] Yield of aniline. [u] Yield of *N*-methylaniline. [v] Catalyst (50 mg).

demonstrate that this hydrogenative heterogeneous catalytic protocol that makes use of catalyst Pd–In_2O_3 (5.3 wt%) offers an environmentally benign alternative to the stoichiometric methods traditionally used to liberate aromatic amines protected as acetamides.[55] A mixture of the methylated and the primary aniline was obtained by using *N*-phenylformamide and *N*,*N*′-diphenylurea as reactants (Table 2, entries 18 and 19). Moreover, aliphatic amides were also suitable substrates to accomplish the C–N bond cleavage efficiently. Morpholine was afforded in a quantitative yield by hydrogenation of 4-acetylmorpholine (Table 2, entry 20), and alkyl and branched primary amides, such as butyramide and cyclohexanecarboxamide, were hydrogenated to give their corresponding aliphatic alcohols in 89 and 85% yields, respectively (Table 2, entries 21 and 22).

To our pleasant surprise, the hydrogenation of the cyclic amides 1-phenyl-2-pyrrolidinone and ε-caprolactam renders their corresponding cyclic amines in excellent yields (Scheme 2). Results shown in Table 2 and the detection of 2-(phenylamino)ethan-1-ol as an intermediate during the course of the hydrogenation of 1-phenyl-2-pyrrolidinone suggest that the reaction mechanism for the formation of cyclic amines also proceeds through hydrogenative C–N bond cleavage to form, firstly, the corresponding aminoalcohols, followed by cyclization that is likely driven by the ring stabilization energy. Indeed, the reaction of 6-amino-1-hexanol under otherwise the same conditions as those used for the hydrogenation of ε-caprolactam achieved cyclic hexamethyleneimine in good yield (see Scheme S2 in the ESI†).

Conclusions

In summary, we have prepared a series of Pd-doped In_2O_3-based materials by a microwave hydrothermal-assisted method combined with a calcination treatment. Their structural and morphological characterization reveals the formation of the body-centered cubic (bcc)-In_2O_3 structure and the successful insertion of Pd(II) cationic species inside the oxide matrix of In_2O_3. The resulting materials are efficient catalysts for the selective hydrogenation of amides to their corresponding alcohols and amines. Their catalytic performance relies on the degree of the Pd-doping and, more specifically, on the relative content of Pd^{2+} cationic species, which mainly vanish during the reaction and can be easily recovered by a rapid annealing treatment.

Application of a prepared highly active Pd-doped In_2O_3 catalyst allows for the development of the first general heterogeneous catalytic protocol for the hydrogenative C–N bond cleavage of a wide range of amides. Structurally different primary, secondary and tertiary amides, including both aromatic and aliphatic ones, are efficiently hydrogenated to produce alcohols and amines in good to excellent yields. Notably, cyclic amides give access to their corresponding cyclic amines. Compared to previously reported heterogeneous catalytic systems for this reaction, the Pd-doped In_2O_3 catalyst presented herein has important advantages of working under additive-free conditions and without promoting dearomatization during the hydrogenation reactions. Therefore, this superior catalyst could find increasing applications on both the academic and the industrial scale for the production of alcohols and amines, as well as in organic synthetic deprotection methodologies.

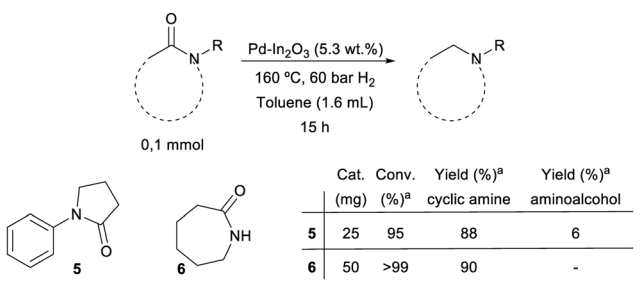

	Cat. (mg)	Conv. (%)[a]	Yield (%)[a] cyclic amine	Yield (%)[a] aminoalcohol
5	25	95	88	6
6	50	>99	90	-

Scheme 2 Hydrogenation of cyclic amides with catalyst Pd–In_2O_3 (5.3 wt%). [a]Determined by GC using *n*-hexadecane as an internal standard

Experimental details

Synthesis of Pd-doped In_2O_3 catalysts

Catalyst preparation was performed by a microwave hydrothermal-assisted method followed by a rapid calcination process. Various amounts of $PdCl_2$, previously dispersed in 1.5 mL of HNO_3 at 160 °C for 30 min, were added to a solution of $In(CH_3CO_2)_3$ in 40 mL of distilled H_2O under vigorous stirring. Then, the pH was adjusted to 12.0 by adding dropwise an aqueous KOH solution (3 M). This mixture was transferred to an autoclave, sealed and heated at 140 °C under static conditions for 8 min with a heating rate of 5 °C min^{-1} in a microwave-hydrothermal equipment. After cooling down to reaction temperature, the precipitate powder was separated by decantation, washed with distilled water and ethanol, and dispersed again in this organic solvent to be dried under slow evaporation at 60 °C. The final aggregate solid was finely ground and annealed at 400 °C for 2 min in a conventional oven (5 °C min^{-1}) to obtain In_2O_3-based materials with different degrees of palladium doping (0, 1, 1.5, 3.5 or 5.3 wt%) depending on the amount of $In(CH_3CO_2)_3$ (0.5468, 0.5379, 0.5324, 0.5182 or 0.5042 g) and $PdCl_2$ (0, 3.3, 9.9, 19.7 or 29 mg, respectively) used.

General procedure for the hydrogenation of amides

An 8 mL vial containing a stirring bar was charged with the amide substrate (0.1 mmol), the catalyst (15 mg), *n*-hexadecane (25 μL) as an internal standard, and toluene (1.6 mL). The vial was then sealed with a septum cap perforated with an extremely fine syringe needle, and placed on an alloy plate inside a 300 mL stainless steel autoclave vessel. The autoclave was tightly closed and pressurized with hydrogen, firstly purged three times with 30 bar, and then at 60 bar. After the reaction, the autoclave was allowed to cool down to room temperature and carefully depressurized. The reaction mixture was diluted with ethyl acetate and an

aliquot was taken to be analyzed by GC. To determine the isolated yields, no internal standard was added and the general procedure was scaled up by a factor of five. After reaction completion and dilution with ethyl acetate, the catalyst was separated off by filtration and the solvent was removed under reduced pressure. The final products were purified by column chromatography (silica; *n*-hexane/ethyl acetate mixture = 10 : 1 → 5 : 1).

Conflicts of interest

There are no conflicts to declare.

Acknowledgements

Financial support from the Spanish Ministerio de Ciencia, Innovación y Universidades (project PGC2018-094417-B-I00) and Universitat Jaume I (UJI-B2016-25) is gratefully acknowledged. I. S. thanks the Spanish Ministerio de Economía, Industria y Competitividad for a postdoctoral "Juan de la Cierva-Incorporación" fellowship (IJCI-2016-30590). S. C. S. L. would like to thank the Coordenacão de Aperfeiçoamento de Pessoal de Nivel Superior (CAPES) for the predoctoral and PDSE (Process 88881.187798/2018-01) fellowships. R. C. L. acknowledges financial support from the Coordenação de Aperfeiçoamento de Pessoal de Nível Superior (CAPES), Conselho Nacional de Desenvolvimento Científico e Tecnologico (CNPq), Fundação de Amparo a Pesquisa do Estado de Minas Gerais (FAPEMIG) and Grupo de Materiais Inorgânicos do Triângulo (GMIT) – Research Group supported by FAPEMIG (APQ-00330-14). S. M. acknowledges DGA/fondos FEDER (construyendo Europa desde Aragón) for funding the research group Platón (E31_17R). A. M. acknowledges the Centre for High-resolution Electron Microscopy (*ChEM*), supported by SPST of ShanghaiTech University under contract No. EM02161943, and the Natural National Science Foundation of China under the grants NFSC-21850410448 and NSFC-21835002. The authors also thank the Serveis Centrals d'Instrumentació Cientifica (SCIC) of the Universitat Jaume I for providing us access to XRD and NMR instruments, as well as Dr. G. Antorrena for technical support in the XPS studies.

References

1 (*a*) P. Roose, K. Eller, E. Henkes, R. Rossbacher and H. Höke, in *Ullmann's Encyclopedia of Industrial Chemistry*, Wiley-VCH Verlag GmbH & Co, Germany, 2000; (*b*) H. A. Wittcoff, B. G. Reuben and J. S. Plotkin, in *Industrial Organic Chemicals*, John Wiley & Sons, Inc., New Jersey, 2nd edn, 2013; (*c*) P. A. Dub and T. Ikariya, *ACS Catal.*, 2012, **2**, 1718–1741; (*d*) S. Werkmeister, K. Junge and M. Beller, *Org. Process Res. Dev.*, 2014, **18**, 289–302; (*e*) J. Pritchard, G. A. Filonenko, R. van Putten, E. J. M. Hensen and E. A. Pidko, *Chem. Soc. Rev.*, 2015, **44**, 3808–3833.

2 (*a*) A. M. Smith and R. Whyman, *Chem. Rev.*, 2014, **114**, 5477–5510; (*b*) A. Chardon, E. Morisset, J. Rouden and J. Blanchet, *Synthesis*, 2018, **50**, 984–997.

3 (*a*) G. W. Gribble and P. W. Heald, *Synthesis*, 1975, 650–652; (*b*) P. Marchini, G. Liso, A. Reho, F. Liberatore and F. M. Moracci, *J. Org. Chem.*, 1975, **40**, 3453–3456; (*c*) G. W. Gribble, J. M. Jasinski, J. T. Pellicone and J. A. Panetta, *Synthesis*, 1978, 766–768; (*d*) G. Trapani, A. Reho and A. Latrofa, *Synthesis*, 1983, 1013–1014; (*e*) C. Perrio-Huard, C. Aubert and M. C. Lasne, *J. Chem. Soc., Perkin Trans. 1*, 2000, 311–316; (*f*) I. Sorribes, K. Junge and M. Beller, *Chem. – Eur. J.*, 2014, **20**, 7878–7883; (*g*) S. Savourey, G. Lefevre, J.-C. Berthet and T. Cantat, *Chem. Commun.*, 2014, **50**, 14033–14036; (*h*) I. Sorribes, K. Junge and M. Beller, *J. Am. Chem. Soc.*, 2014, **136**, 14314–14319; (*i*) I. Sorribes, K. Junge and M. Beller, *J. Am. Chem. Soc.*, 2015, **137**, 2138–2138; (*j*) I. Sorribes, J. R. Cabrero-Antonino, C. Vicent, K. Junge and M. Beller, *J. Am. Chem. Soc.*, 2015, **137**, 13580–13587; (*k*) Y. Li, I. Sorribes, C. Vicent, K. Junge and M. Beller, *Chem. – Eur. J.*, 2015, **21**, 16759–16763; (*l*) M.-C. Fu, R. Shang, W.-M. Cheng and Y. Fu, *Angew. Chem., Int. Ed.*, 2015, **54**, 9042–9046; (*m*) J. R. Cabrero-Antonino, R. Adam, K. Junge and M. Beller, *Catal. Sci. Technol.*, 2016, **6**, 7956–7966; (*n*) K. G. Andrews, D. M. Summers, L. J. Donnelly and R. M. Denton, *Chem. Commun.*, 2016, **52**, 1855–1858; (*o*) M. Minakawa, M. Okubo and M. Kawatsura, *Tetrahedron Lett.*, 2016, **57**, 4187–4190; (*p*) L. Zhu, L.-S. Wang, B. Li, W. Li and B. Fu, *Catal. Sci. Technol.*, 2016, **6**, 6172–6176; (*q*) Y. Shi, P. C. J. Kamer and D. J. Cole-Hamilton, *Green Chem.*, 2017, **19**, 5460–5466; (*r*) E. Pedrajas, I. Sorribes, E. Guillamon, K. Junge, M. Beller and R. Llusar, *Chem. – Eur. J.*, 2017, **23**, 13205–13212; (*s*) C. Qiao, X.-F. Liu, X. Liu and L.-N. He, *Org. Lett.*, 2017, **19**, 1490–1493; (*t*) C. Qiao, X.-Y. Yao, X.-F. Liu, H.-R. Li and L.-N. He, *Asian J. Org. Chem.*, 2018, **7**, 1815–1818; (*u*) W. Liu, B. Sahoo, A. Spannenberg, K. Junge and M. Beller, *Angew. Chem., Int. Ed.*, 2018, **57**, 11673–11677; (*v*) J. R. Cabrero-Antonino, R. Adam and M. Beller, *Angew. Chem., Int. Ed.*, 2019, **58**, 12820–12838.

4 (*a*) O. Jacquet, X. Frogneux, C. D. N. Gomes and T. Cantat, *Chem. Sci.*, 2013, **4**, 2127–2131; (*b*) Y. Li, X. Fang, K. Junge and M. Beller, *Angew. Chem., Int. Ed.*, 2013, **52**, 9568–9571; (*c*) K. Beydoun, T. vom Stein, J. Klankermayer and W. Leitner, *Angew. Chem., Int. Ed.*, 2013, **52**, 9554–9557; (*d*) Y. Li, I. Sorribes, T. Yan, K. Junge and M. Beller, *Angew. Chem., Int. Ed.*, 2013, **52**, 12156–12160; (*e*) S. Das, F. D. Bobbink, G. Laurenczy and P. J. Dyson, *Angew. Chem., Int. Ed.*, 2014, **53**, 12876–12879; (*f*) E. Blondiaux, J. Pouessel and T. Cantat, *Angew. Chem., Int. Ed.*, 2014, **53**, 12186–12190; (*g*) X. Cui, Y. Zhang, Y. Deng and F. Shi, *Chem. Commun.*, 2014, **50**, 13521–13524; (*h*) X. Cui, X. Dai, Y. Zhang, Y. Deng and F. Shi, *Chem. Sci.*, 2014, **5**, 649–655; (*i*) A. Tlili, E. Blondiaux, X. Frogneux and T. Cantat, *Green Chem.*, 2015, **17**, 157–168; (*j*) Q. Liu, L. Wu, R. Jackstell and M. Beller, *Nat. Commun.*, 2015, **6**, 5933; (*k*) X.-L. Du, G. Tang, H.-L. Bao, Z. Jiang, X.-H. Zhong, D. S. Su and J.-Q. Wang, *ChemSusChem*, 2015, **8**, 3489–3496; (*l*) J. Klankermayer, S. Wesselbaum, K. Beydoun and W. Leitner, *Angew. Chem., Int. Ed.*, 2016, **55**, 7296–7343; (*m*) Y. Li, X. Cui, K. Dong, K. Junge and M. Beller, *ACS Catal.*, 2017, **7**, 1077–1086; (*n*) X.-D. Li, S.-M. Xia, K.-H.

Chen, X.-F. Liu, H.-R. Li and L.-N. He, *Green Chem.*, 2018, **20**, 4853–4858; (*o*) J. Artz, T. E. Müller, K. Thenert, J. Kleinekorte, R. Meys, A. Sternberg, A. Bardow and W. Leitner, *Chem. Rev.*, 2018, **118**, 434–504; (*p*) R. H. Lam, C. M. A. McQueen, I. Pernik, R. T. McBurney, A. F. Hill and B. A. Messerle, *Green Chem.*, 2019, **21**, 538–549; (*q*) S. Dabral and T. Schaub, *Adv. Synth. Catal.*, 2019, **361**, 223–246; (*r*) Y. Yang and J.-W. Lee, *Chem. Sci.*, 2019, **10**, 3905–3926.

5 J. Seyden-Penne, in *Reductions by the Alumino and borohydrides in Organic Synthesis*, Wiley-VCH, New York, 2nd edn, 1997.

6 (*a*) M. Szostak, M. Spain, A. J. Eberhart and D. J. Procter, *J. Am. Chem. Soc.*, 2014, **136**, 2268–2271; (*b*) S. R. Huq, S. Shi, R. Diao and M. Szostak, *J. Org. Chem.*, 2017, **82**, 6528–6540.

7 B. Zhang, H. Li, Y. Ding, Y. Yan and J. An, *J. Org. Chem.*, 2018, **83**, 6006–6014.

8 D. Y. Ong, Z. Yen, A. Yoshii, J. Revillo Imbernon, R. Takita and S. Chiba, *Angew. Chem., Int. Ed.*, 2019, **58**, 4992–4997.

9 (*a*) S. Zhou, K. Junge, D. Addis, S. Das and M. Beller, *Angew. Chem., Int. Ed.*, 2009, **48**, 9507–9510; (*b*) S. Das, D. Addis, S. Zhou, K. Junge and M. Beller, *J. Am. Chem. Soc.*, 2010, **132**, 1770–1771; (*c*) S. Das, D. Addis, K. Junge and M. Beller, *Chem. – Eur. J.*, 2011, **17**, 12186–12192; (*d*) D. Addis, S. Das, K. Junge and M. Beller, *Angew. Chem., Int. Ed.*, 2011, **50**, 6004–6011; (*e*) Y. Mikami, A. Noujima, T. Mitsudome, T. Mizugaki, K. Jitsukawa and K. Kaneda, *Chem. – Eur. J.*, 2011, **17**, 1768–1772; (*f*) S. Das, B. Join, K. Junge and M. Beller, *Chem. Commun.*, 2012, **48**, 2683–2685; (*g*) S. Das, B. Wendt, K. Möller, K. Junge and M. Beller, *Angew. Chem., Int. Ed.*, 2012, **51**, 1662–1666; (*h*) S. Park and M. Brookhart, *J. Am. Chem. Soc.*, 2012, **134**, 640–653; (*i*) C. Cheng and M. Brookhart, *J. Am. Chem. Soc.*, 2012, **134**, 11304–11307; (*j*) J. T. Reeves, Z. Tan, M. A. Marsini, Z. S. Han, Y. Xu, D. C. Reeves, H. Lee, B. Z. Lu and C. H. Senanayakea, *Adv. Synth. Catal.*, 2013, **355**, 47–52; (*k*) T. Dombray, C. Helleu, C. Darcel and J.-B. Sortais, *Adv. Synth. Catal.*, 2013, **355**, 3358–3362; (*l*) Y. Li, J. A. Molina de La Torre, K. Grabow, U. Bentrup, K. Junge, S. Zhou, A. Brückner and M. Beller, *Angew. Chem., Int. Ed.*, 2013, **52**, 11577–11580; (*m*) E. Blondiaux and T. Cantat, *Chem. Commun.*, 2014, **50**, 9349–9352; (*n*) R. C. Chadwick, V. Kardelis, P. Lim and A. Adronov, *J. Org. Chem.*, 2014, **79**, 7728–7733; (*o*) S. Das, Y. Li, C. Bornschein, S. Pisiewicz, K. Kiersch, D. Michalik, F. Gallou, K. Junge and M. Beller, *Angew. Chem., Int. Ed.*, 2015, **54**, 12389–12393; (*p*) D. S. Mérel, M. L. T. Do, S. Gaillard, P. Dupau and J.-L. Renaud, *Coord. Chem. Rev.*, 2015, **288**, 50–68; (*q*) F. Tinnis, A. Volkov, T. Slagbrand and H. Adolfsson, *Angew. Chem., Int. Ed.*, 2016, **55**, 4562–4566; (*r*) S. Das, Y. Li, L.-Q. Lu, K. Junge and M. Beller, *Chem. – Eur. J.*, 2016, **22**, 7050–7053; (*s*) B. Li, J.-B. Sortais and C. Darcel, *RSC Adv.*, 2016, **6**, 57603–57625; (*t*) A. Volkov, F. Tinnis, T. Slagbrand, P. Trillo and H. Adolfsson, *Chem. Soc. Rev.*, 2016, **45**, 6685–6697; (*u*) P.-Q. Huang, Q.-W. Lang and Y.-R. Wang, *J. Org. Chem.*, 2016, **81**, 4235–4243; (*v*) A. Chardon, T. Mohy El Dine, R. Legay, M. De Paolis, J. Rouden and J. Blanchet, *Chem. – Eur. J.*, 2017, **23**, 2005–2009; (*w*) C. M. Kelly, R. McDonald, O. L. Sydora, M. Stradiotto and L. Turculet, *Angew. Chem., Int. Ed.*, 2017, **56**, 15901–15904; (*x*) Y. Corre, X. Trivelli, F. Capet, J.-P. Djukic, F. Agbossou-Niedercorn and C. Michon, *ChemCatChem*, 2017, **9**, 2009–2017; (*y*) H. Li, W. Zhao, W. Dai, J. Long, M. Watanabe, S. Meier, S. Saravanamurugan, S. Yang and A. Riisager, *Green Chem.*, 2018, **20**, 5327–5335; (*z*) A. Nurseiit, J. Janabel, K. A. Gudun, A. Kassymbek, M. Segizbayev, T. M. Seilkhanov and A. Y. Khalimon, *ChemCatChem*, 2019, **11**, 790–798; (*aa*) M. Iglesias, F. J. Fernández-Alvarez and L. A. Oro, *Coord. Chem. Rev.*, 2019, **386**, 240–266.

10 (*a*) N. L. Lampland, M. Hovey, D. Mukherjee and A. D. Sadow, *ACS Catal.*, 2015, **5**, 4219–4226; (*b*) D. Mukherjee, S. Shirase, T. P. Spaniol, K. Mashima and J. Okuda, *Chem. Commun.*, 2016, **52**, 13155–13158; (*c*) Y. Pan, Z. Luo, J. Han, X. Xu, C. Chen, H. Zhao, L. Xu, Q. Fan and J. Xiao, *Adv. Synth. Catal.*, 2019, **361**, 2301–2308.

11 Y. Pan, Z. Luo, X. Xu, H. Zhao, J. Han, L. Xu, Q. Fan and J. Xiao, *Adv. Synth. Catal.*, 2019, **361**, 3800–3806.

12 (*a*) P. J. Dunn, K. K. Hii, M. J. Krische and M. T. Williams, in *Sustainable Catalysis: Challenges and Practices for the Pharmaceutical and Fine Chemical Industries*, John Wiley and Sons, Inc, Hoboken, New Jersey, 2013; (*b*) S. G. Koenig, D. K. Leahy and A. S. Wells, *Org. Process Res. Dev.*, 2018, **22**, 1344–1359; (*c*) M. C. Bryan, P. J. Dunn, D. Entwistle, F. Gallou, S. G. Koenig, J. D. Hayler, M. R. Hickey, S. Hughes, M. E. Kopach, G. Moine, P. Richardson, F. Roschangar, A. Steven and F. J. Weiberth, *Green Chem.*, 2018, **20**, 5082–5103.

13 (*a*) D. Cantillo, *Eur. J. Inorg. Chem.*, 2011, **2011**, 3008–3013; (*b*) H. Li and M. B. Hall, *ACS Catal.*, 2015, **5**, 1895–1913.

14 (*a*) A. Suarez, *Phys. Sci. Rev.*, 2018, **3**, 183–229; (*b*) A. Suarez, in *Hydrogenation of carbonyl compounds of relevance to hydrogen storage in alcohols*, Walter de Gruyter GMBH, Berlin, 2019.

15 (*a*) H. Adkins and B. Wojcik, *J. Am. Chem. Soc.*, 1934, **56**, 247–247; (*b*) B. Wojcik and H. Adkins, *J. Am. Chem. Soc.*, 1934, **56**, 2419–2424; (*c*) J. D. D'Ianni and H. Adkins, *J. Am. Chem. Soc.*, 1939, **61**, 1675–1681; (*d*) H. J. Schneider, H. Adkins and S. M. McElvain, *J. Am. Chem. Soc.*, 1952, **74**, 4287–4290.

16 H. S. Broadbent and W. J. Bartley, *J. Org. Chem.*, 1963, **28**, 2345–2347.

17 A. Guyer, A. Bieler and G. Gerliczy, *Helv. Chim. Acta*, 1955, **38**, 1649–1654.

18 F. Galinovsky and E. Stern, *Ber. Dtsch. Chem. Ges.*, 1943, **76**, 1034–1038.

19 I. A. Dobson, EP-0286280, BP Chemicals Limited, 1988.

20 C. Hirosawa, N. Wakasa and T. Fuchikami, *Tetrahedron Lett.*, 1996, **37**, 6749–6752.

21 G. Beamson, A. J. Papworth, C. Philipps, A. M. Smith and R. Whyman, *Adv. Synth. Catal.*, 2010, **352**, 869–883.

22 (*a*) G. Beamson, A. J. Papworth, C. Philipps, A. M. Smith and R. Whyman, *J. Catal.*, 2010, **269**, 93–102; (*b*) A. M. Maj, I. Suisse, N. Pinault, N. Robert and F. Agbossou-Niedercorn, *ChemCatChem*, 2014, **6**, 2621–2625; (*c*) Y. Nakagawa, R. Tamura, M. Tamura and K. Tomishige, *Sci. Technol. Adv. Mater.*, 2015, **16**, 014901–014901.

23 G. Beamson, A. J. Papworth, C. Philipps, A. M. Smith and R. Whyman, *J. Catal.*, 2011, **278**, 228–238.

24 (*a*) R. Burch, C. Paun, X. M. Cao, P. Crawford, P. Goodrich, C. Hardacre, P. Hu, L. McLaughlin, J. Sá and J. M. Thompson, *J. Catal.*, 2011, **283**, 89–97; (*b*) J. Coetzee, H. G. Manyar, C. Hardacre and D. J. Cole-Hamilton, *ChemCatChem*, 2013, **5**, 2843–2847.

25 M. Stein and B. Breit, *Angew. Chem., Int. Ed.*, 2013, **52**, 2231–2234.

26 S. Li, H. Chen, M. Wen and J. Shen, *J. Catal.*, 2016, **338**, 1–11.

27 K.-i. Shimizu, W. Onodera, A. S. Touchy, S. M. A. H. Siddiki, T. Toyao and K. Kon, *ChemistrySelect*, 2016, **1**, 736–740.

28 T. Chen, Z. Shi, G. Zhang, H. C. Chan, Y. Shu, Q. Gao and Y. Tang, *ACS Appl. Mater. Interfaces*, 2018, **10**, 42475–42483.

29 A. A. Smith, P. Dani, P. D. Higginson and A. J. Pettman, WO-2005066112, Avantium International B.V., 2005.

30 T. Mitsudome, K. Miyagawa, Z. Maeno, T. Mizugaki, K. Jitsukawa, J. Yamasaki, Y. Kitagawa and K. Kaneda, *Angew. Chem., Int. Ed.*, 2017, **56**, 9381–9385.

31 T. Toyao, S. M. A. H. Siddiki, Y. Morita, T. Kamachi, A. S. Touchy, W. Onodera, K. Kon, S. Furukawa, H. Ariga, K. Asakura, K. Yoshizawa and K.-i. Shimizu, *Chem. – Eur. J.*, 2017, **23**, 14848–14859.

32 (*a*) A. A. Núñez Magro, G. R. Eastham and D. J. Cole-Hamilton, *Chem. Commun.*, 2007, 3154–3156; (*b*) J. Coetzee, D. L. Dodds, J. Klankermayer, S. Brosinski, W. Leitner, A. M. Z. Slawin and D. J. Cole-Hamilton, *Chem. – Eur. J.*, 2013, **19**, 11039–11050; (*c*) M. Meuresch, S. Westhues, W. Leitner and J. Klankermayer, *Angew. Chem., Int. Ed.*, 2016, **55**, 1392–1395; (*d*) M.-L. Yuan, J.-H. Xie and Q.-L. Zhou, *ChemCatChem*, 2016, **8**, 3036–3040; (*e*) J. R. Cabrero-Antonino, E. Alberico, K. Junge, H. Junge and M. Beller, *Chem. Sci.*, 2016, **7**, 3432–3442; (*f*) S. Westhues, M. Meuresch and J. Klankermayer, *Angew. Chem., Int. Ed.*, 2016, **55**, 12841–12844.

33 M.-L. Yuan, J.-H. Xie, S.-F. Zhu and Q.-L. Zhou, *ACS Catal.*, 2016, **6**, 3665–3669.

34 Y.-Q. Zou, S. Chakraborty, A. Nerush, D. Oren, Y. Diskin-Posner, Y. Ben-David and D. Milstein, *ACS Catal.*, 2018, **8**, 8014–8019.

35 (*a*) M. Ito, A. Sakaguchi, C. Kobayashi and T. Ikariya, *J. Am. Chem. Soc.*, 2007, **129**, 290–291; (*b*) M. Ito, L. W. Koo, A. Himizu, C. Kobayashi, A. Sakaguchi and T. Ikariya, *Angew. Chem., Int. Ed.*, 2009, **48**, 1324–1327; (*c*) M. Ito, C. Kobayashi, A. Himizu and T. Ikariya, *J. Am. Chem. Soc.*, 2010, **132**, 11414–11415; (*d*) E. Balaraman, B. Gnanaprakasam, L. J. W. Shimon and D. Milstein, *J. Am. Chem. Soc.*, 2010, **132**, 16756–16758; (*e*) M. Ito, T. Ootsuka, R. Watari, A. Shiibashi, A. Himizu and T. Ikariya, *J. Am. Chem. Soc.*, 2011, **133**, 4240–4242; (*f*) J. M. John and S. H. Bergens, *Angew. Chem., Int. Ed.*, 2011, **50**, 10377–10380; (*g*) T. Miura, I. E. Held, S. Oishi, M. Naruto and S. Saito, *Tetrahedron Lett.*, 2013, **54**, 2674–2678; (*h*) Y. Kita, T. Higuchi and K. Mashima, *Chem. Commun.*, 2014, **50**, 11211–11213; (*i*) T. Ikariya and Y. Kayaki, *Pure Appl. Chem.*, 2014, **86**, 933; (*j*) J. M. John, R. Loorthuraja, E. Antoniuk and S. H. Bergens, *Catal. Sci. Technol.*, 2015, **5**, 1181–1186; (*k*) J. A. Garg, S. Chakraborty, Y. Ben-David and D. Milstein, *Chem. Commun.*, 2016, **52**, 5285–5288; (*l*) J. R. Cabrero-Antonino, E. Alberico, H.-J. Drexler, W. Baumann, K. Junge, H. Junge and M. Beller, *ACS Catal.*, 2016, **6**, 47–54; (*m*) N. M. Rezayee, D. C. Samblanet and M. S. Sanford, *ACS Catal.*, 2016, **6**, 6377–6383; (*n*) F. Schneck, M. Assmann, M. Balmer, K. Harms and R. Langer, *Organometallics*, 2016, **35**, 1931–1943; (*o*) L. Rasu, J. M. John, E. Stephenson, R. Endean, S. Kalapugama, R. Clément and S. H. Bergens, *J. Am. Chem. Soc.*, 2017, **139**, 3065–3071; (*p*) T. Miura, M. Naruto, K. Toda, T. Shimomura and S. Saito, *Sci. Rep.*, 2017, **7**, 1586; (*q*) L. Shi, X. Tan, J. Long, X. Xiong, S. Yang, P. Xue, H. Lv and X. Zhang, *Chem. – Eur. J.*, 2017, **23**, 546–548; (*r*) V. Papa, J. R. Cabrero-Antonino, E. Alberico, A. Spanneberg, K. Junge, H. Junge and M. Beller, *Chem. Sci.*, 2017, **8**, 3576–3585; (*s*) U. Jayarathne, Y. Zhang, N. Hazari and W. H. Bernskoetter, *Organometallics*, 2017, **36**, 409–416; (*t*) Z. Wang, Y. Li, Q.-b. Liu, G. A. Solan, Y. Ma and W.-H. Sun, *ChemCatChem*, 2017, **9**, 4275–4281; (*u*) L. Artús Suàrez, Z. Culakova, D. Balcells, W. H. Bernskoetter, O. Eisenstein, K. I. Goldberg, N. Hazari, M. Tilset and A. Nova, *ACS Catal.*, 2018, **8**, 8751–8762; (*v*) J. Chen, J. Wang and T. Tu, *Chem. – Asian J.*, 2018, **13**, 2559–2565; (*w*) T. Kawano, R. Watari, Y. Kayaki and T. Ikariya, *Synthesis*, 2019, **51**, 2542–2547; (*x*) T. Leischner, L. Artús Suarez, A. Spannenberg, K. Junge, A. Nova and M. Beller, *Chem. Sci.*, 2019, DOI: 10.1039/C9SC03453F.

36 Y. Xie, P. Hu, T. Bendikov and D. Milstein, *Catal. Sci. Technol.*, 2018, **8**, 2784–2788.

37 M. Tamura, S. Ishikawa, M. Betchaku, Y. Nakagawa and K. Tomishige, *Chem. Commun.*, 2018, **54**, 7503–7506.

38 (*a*) K. Sun, Z. Fan, J. Ye, J. Yan, Q. Ge, Y. Li, W. He, W. Yang and C.-j. Liu, *J. CO2 Util.*, 2015, **12**, 1–6; (*b*) O. Martin, A. J. Martín, C. Mondelli, S. Mitchell, T. F. Segawa, R. Hauert, C. Drouilly, D. Curulla-Ferré and J. Pérez-Ramírez, *Angew. Chem., Int. Ed.*, 2016, **55**, 6261–6265; (*c*) M. S. Frei, M. Capdevila-Cortada, R. García-Muelas, C. Mondelli, N. López, J. A. Stewart, D. Curulla Ferré and J. Pérez-Ramírez, *J. Catal.*, 2018, **361**, 313–321.

39 (*a*) Q. Sun, J. Ye, C.-J. Liu and Q. Ge, *Greenhouse Gases: Sci. Technol.*, 2014, **4**, 140–144; (*b*) W. Wang, Y. Zhang, Z. Wang, J.-M. Yan, Q. Ge and C.-J. Liu, *Catal. Today*, 2016, **259**, 402–408; (*c*) E.-M. Köck, M. Kogler, M. Grünbacher, C. Zhuo, R. Thalinger, D. Schmidmair, L. Schlicker, A. Gurlo and S. Penner, *J. Phys. Chem. C*, 2016, **120**, 15272–15281.

40 J. Wang, A. Zhang, X. Jiang, C. Song and X. Guo, *J. CO2 Util.*, 2018, **27**, 81–88.

41 J. Su, D. Wang, Y. Wang, H. Zhou, C. Liu, S. Liu, C. Wang, W. Yang, Z. Xie and M. He, *ChemCatChem*, 2018, **10**, 1536–1541.

42 (*a*) N. S. Smirnova, D. A. Shlyapin, O. V. Protasova, M. V. Trenikhin, T. I. Gulyaeva, E. Y. Gerasimov, L. S. Kibis, N. B. Shitova, D. I. Kochubey and P. G. Tsyrul'nikov, *Chem. Sustainable Dev.*, 2013, 91–100; (*b*) D. Albani, M. Capdevila-Cortada, G. Vilé, S. Mitchell, O. Martin, N. López and J.

Pérez-Ramírez, *Angew. Chem., Int. Ed.*, 2017, **56**, 10755–10760.

43 H. Lyu, J. Liu, Y. Chen, G. Li, H. Jiang and M. Zhang, *Phys. Chem. Chem. Phys.*, 2018, **20**, 7156–7166.

44 (*a*) J. Ye, C. Liu and Q. Ge, *J. Phys. Chem. C*, 2012, **116**, 7817–7825; (*b*) J. Ye, C. Liu, D. Mei and Q. Ge, *ACS Catal.*, 2013, **3**, 1296–1306; (*c*) M. Dou, M. Zhang, Y. Chen and Y. Yu, *Comput. Theor. Chem.*, 2018, **1126**, 7–15; (*d*) M. Zhang, M. Dou and Y. Yu, *Appl. Surf. Sci.*, 2018, **433**, 780–789; (*e*) M. Zhang, W. Wang and Y. Chen, *Appl. Surf. Sci.*, 2018, **434**, 1344–1352; (*f*) M. Dou, M. Zhang, Y. Chen and Y. Yu, *New J. Chem.*, 2018, **42**, 3293–3300; (*g*) M. Dou, M. Zhang, Y. Chen and Y. Yu, *Surf. Sci.*, 2018, **672**, 7–12.

45 (*a*) T. Bielz, H. Lorenz, W. Jochum, R. Kaindl, F. Klauser, B. Klötzer and S. Penner, *J. Phys. Chem. C*, 2010, **114**, 9022–9029; (*b*) T. Bielz, H. Lorenz, P. Amann, B. Klötzer and S. Penner, *J. Phys. Chem. C*, 2011, **115**, 6622–6628.

46 (*a*) T. Zhang, F. Gu, D. Han, Z. Wang and G. Guo, *Sens. Actuators, B*, 2013, **177**, 1180–1188; (*b*) W.-H. Zhang, F. Wang and W.-D. Zhang, *Dalton Trans.*, 2013, **42**, 4361–4364; (*c*) S. C. S. Lemos, F. C. Romeiro, L. F. de Paula, R. F. Gonçalves, A. P. de Moura, M. M. Ferrer, E. Longo, A. O. T. Patrocinio and R. C. Lima, *J. Solid State Chem.*, 2017, **249**, 58–63; (*d*) H. Ouacha, U. Kleineberg and H. Albrithen, *J. Phys. D: Appl. Phys.*, 2017, **50**, 455102; (*e*) Y. Keriti, A. Keffous, K. Dib, S. Djellab and M. Trari, *Res. Chem. Intermed.*, 2018, **44**, 1537–1550; (*f*) M. Dou, M. Zhang, Y. Chen and Y. Yu, *Catal. Lett.*, 2018, **148**, 3723–3731; (*g*) A. T. Apostolov, I. N. Apostolova and J. M. Wesselinowa, *J. Magn. Magn. Mater.*, 2018, **456**, 263–268; (*h*) J. Xu, J.-B. Liu, B.-X. Liu, S.-N. Li, S.-H. Wei and B. Huang, *Adv. Electron. Mater.*, 2018, **4**, 1700553; (*i*) Y. Keriti, A. Keffous, N. Gabouze and M. Trari, *Optik*, 2019, **176**, 419–424.

47 (*a*) H. Lorenz, S. Turner, O. I. Lebedev, G. Van Tendeloo, B. Klötzer, C. Rameshan, K. Pfaller and S. Penner, *Appl. Catal., A*, 2010, **374**, 180–188; (*b*) J. Ye, C.-j. Liu, D. Mei and Q. Ge, *J. Catal.*, 2014, **317**, 44–53; (*c*) M. Neumann, D. Teschner, A. Knop-Gericke, W. Reschetilowski and M. Armbrüster, *J. Catal.*, 2016, **340**, 49–59; (*d*) N. Rui, Z. Wang, K. Sun, J. Ye, Q. Ge and C.-j. Liu, *Appl. Catal., B*, 2017, **218**, 488–497; (*e*) L. Schlicker, M. F. Bekheet, A. Gili, A. Doran, A. Gurlo, K. Ploner, T. Schachinger and S. Penner, *J. Solid State Chem.*, 2018, **266**, 93–99; (*f*) A. García-Trenco, A. Regoutz, E. R. White, D. J. Payne, M. S. P. Shaffer and C. K. Williams, *Appl. Catal., B*, 2018, **220**, 9–18; (*g*) J. L. Snider, V. Streibel, M. A. Hubert, T. S. Choksi, E. Valle, D. C. Upham, J. Schumann, M. S. Duyar, A. Gallo, F. Abild-Pedersen and T. F. Jaramillo, *ACS Catal.*, 2019, **9**, 3399–3412.

48 (*a*) S. Komarneni, R. Roy and Q. H. Li, *Mater. Res. Bull.*, 1992, **27**, 1393–1405; (*b*) F. C. Romeiro, J. Z. Marinho, A. C. A. Silva, N. F. Cano, N. O. Dantas and R. C. Lima, *J. Phys. Chem. C*, 2013, **117**, 26222–26227; (*c*) F. C. Romeiro, J. Z. Marinho, S. C. S. Lemos, A. P. de Moura, P. G. Freire, L. F. da Silva, E. Longo, R. A. A. Munoz and R. C. Lima, *J. Solid State Chem.*, 2015, **230**, 343–349.

49 F. V. Motta, R. C. Lima, A. P. A. Marques, M. S. Li, E. R. Leite, J. A. Varela and E. Longo, *J. Alloys Compd.*, 2010, **497**, L25–L28.

50 (*a*) M. Kaur, N. Jain, K. Sharma, S. Bhattacharya, M. Roy, A. K. Tyagi, S. K. Gupta and J. V. Yakhmi, *Sens. Actuators, B*, 2008, **133**, 456–461; (*b*) H. Zhu, X. Wang, F. Yang and X. Yang, *Cryst. Growth Des.*, 2008, **8**, 950–956; (*c*) W. Yin, J. Su, M. Cao, C. Ni, S. G. Cloutier, Z. Huang, X. Ma, L. Ren, C. Hu and B. Wei, *J. Phys. Chem. C*, 2009, **113**, 19493–19499.

51 M. Kumar, V. N. Singh, F. Singh, K. V. Lakshmi, B. R. Mehta and J. P. Singh, *Appl. Phys. Lett.*, 2008, **92**, 171907.

52 (*a*) I. Kosacki, T. Suzuki, H. U. Anderson and P. Colomban, *Solid State Ionics*, 2002, **149**, 99–105; (*b*) F. Gu, C. Li, D. Han and Z. Wang, *ACS Appl. Mater. Interfaces*, 2018, **10**, 933–942; (*c*) O. M. Berengue, A. D. Rodrigues, C. J. Dalmaschio, A. J. C. Lanfredi, E. R. Leite and A. J. Chiquito, *J. Phys. D: Appl. Phys.*, 2010, **43**, 045401.

53 M. Mehta, N. Kodan, S. Kumar, A. Kaushal, L. Mayrhofer, M. Walter, M. Moseler, A. Dey, S. Krishnamurthy, S. Basu and A. P. Singh, *J. Mater. Chem. A*, 2016, **4**, 2670–2681.

54 (*a*) J. R. McBride, K. C. Hass and W. H. Weber, *Phys. Rev. B*, 1991, **44**, 5016–5028; (*b*) R. Bardhan, H. F. Zarick, A. Schwartzberg and C. L. Pint, *J. Phys. Chem. C*, 2013, **117**, 21558–21568.

55 T. W. Green and P. G. M. Wuts, in *Protective Groups in Organic Synthesis*, Wiley-Interscience, New York, 1999.

